

See discussions, stats, and author profiles for this publication at: <https://www.researchgate.net/publication/231238395>

# Influence of Magnetic Ordering on the Luminescence in a Layered Organic–Inorganic OPV–Ni(II) Compound

ARTICLE *in* CHEMISTRY OF MATERIALS · JUNE 2004

Impact Factor: 8.35 · DOI: 10.1021/cm049792c

CITATIONS

30

READS

32

7 AUTHORS, INCLUDING:



[Aude Demessence](#)

Claude Bernard University Lyon 1

26 PUBLICATIONS 811 CITATIONS

SEE PROFILE



[Olivier Cregut](#)

French National Centre for Scientific Research

76 PUBLICATIONS 1,284 CITATIONS

SEE PROFILE



[M. Drillon](#)

University of Strasbourg

188 PUBLICATIONS 4,143 CITATIONS

SEE PROFILE



[Pierre Rabu](#)

University of Strasbourg

147 PUBLICATIONS 3,081 CITATIONS

SEE PROFILE

# Influence of Magnetic Ordering on the Luminescence in a Layered Organic–Inorganic OPV–Ni(II) Compound

Jean-Michel Rueff,<sup>†</sup> Jean-François Nierengarten,<sup>†,‡</sup> Pierre Gilliot,<sup>†</sup>  
Aude Demessence,<sup>†</sup> Olivier Cregut,<sup>†</sup> Marc Drillon,<sup>†</sup> and Pierre Rabu<sup>\*,†</sup>

*Institut de Physique et Chimie des Matériaux de Strasbourg UMR 7504 CNRS-ULP,  
23, rue du Loess, 67034 Strasbourg, Cedex, France, and Groupe de Chimie des Fullerènes et  
des Systèmes Conjugués, Ecole Européenne de Chimie, Polymères et Matériaux (ECPM),  
25 rue Becquerel, 67087 Strasbourg Cedex 2, France*

*Received February 10, 2004. Revised Manuscript Received April 28, 2004*

Oligophenylenevinylene (OPV) tetracarboxylate luminescent ligand **5** has been synthesized and used for the design of a new Ni(II) layered organic–inorganic compound (**8**) obtained by the reaction of **5** with nickel(II) nitrate hexahydrate. The hybrid compound **8** has been characterized by powder X-ray diffraction and its magnetic and luminescent properties have been investigated as a function of temperature. The structure consists of the stacking of ferromagnetic Ni(II) based layers at ca. 29 Å apart. A ferromagnetic 3D order occurs at  $T_C = 9.5$  K. The study of the temperature dependence of the luminescent properties of the OPV-based hybrid compound shows that the  $\pi$  electron sub-system is influenced by the magnetic ordering of the Ni(II) sub-network.

## Introduction

The design of multi-functional materials combining magnetism and optical activity,<sup>1–4</sup> nonlinear optical properties (NLO),<sup>5,6</sup> or conductivity<sup>7</sup> is an important trend in modern molecular and coordination chemistry. Organic–inorganic (O/I) compounds consisting of the controlled packing of molecular organic and inorganic entities are well suited for providing new systems in which each subnetwork is organized at a nanoscale level and exhibits its own properties.<sup>5,6,8</sup> Striking examples are found in insertion compounds such as MnPS<sub>3</sub> including NLO molecules,<sup>9,10</sup> or layered Mn<sup>II</sup>Cr<sup>III</sup>–oxalate co-crystallized with NLO<sup>11</sup> or TTF-based conducting cations,<sup>7</sup> but synergistic effects have not been demonstrated yet within these classes of multifunctional materials.

Recently, the design of new O/I materials based on divalent transition metal hydroxide layers interleaved

by organic anionic species has been pointed out by anion exchange reactions or hydrothermal synthesis.<sup>12</sup> In that case, the organic entities contribute to the anionic backbone and coordinate the magnetic centers, and strong interactions are observed between the electronic populations attached to each subnetwork.<sup>13</sup>

Correlations were established between the properties and the structures or the nature of the chemical bond in a series of compounds showing that the use of organic molecules is really suitable for tuning the interactions between magnetic entities. When using simple pillars, long range order may occur due to the dipolar interaction between magnetic layers, even when they are far apart. The grafting of difunctional aliphatic or aromatic species enables tuning of the coupling through a polarization mechanism involving the  $\pi$  electron system. Also, strong anisotropy effects have been reported in the case of weak ferromagnetic Co(II) derivatives with huge value of coercive field. More recently, the occurrence of 2D/3D dimensionality crossover has been demonstrated in these systems.<sup>14</sup>

We report here a new transition metal hybrid compound exhibiting both a net magnetic moment and photoluminescence properties due to the presence of magnetic layers and oligophenylenevinylene (OPV) chromophores between these layers. In the design of the organic ligand **1**, it is worth noting that the OPV backbone has been selected for its high luminescence efficiency.<sup>15</sup> Effectively, emission quantum yields close to unity have been observed for short OPV derivatives

\* To whom correspondence should be addressed. Tel: 33 3 88 10 71 35. Fax: 33 3 88 10 72 47. E-mail: pierre.rabu@ipcms.u-strasbg.fr.

<sup>†</sup> Institut de Physique et Chimie des Matériaux de Strasbourg UMR 7504 CNRS-ULP.

<sup>‡</sup> Ecole Européenne de Chimie, Polymères et Matériaux (ECPM).

(1) Rikken, G. L.; Raupach, E. *Nature* **2000**, *405*, 932.

(2) Minguet, M.; Luneau, D.; Lhotel, E.; Villar, V.; Paulsen, C.; Amabilino, D. B.; Veciana, J. *Angew. Chem. Int. Ed.* **2002**, *114*.

(3) Kumagai, H.; Inoue, K. *Angew. Chem. Int. Ed.* **1999**, *38*, 1601.

(4) Barron, L. D. *Nature* **2000**, *504*, 895.

(5) Bénard, S.; Yu, P.; Coradin, T.; Rivière, E.; Nakatani, K.; Clément, R. *Adv. Mater.* **1997**, *9*, 981.

(6) Bénard, S.; Léaustic, A.; Rivière, E.; Yu, P.; Clément, R. *Chem. Mater.* **2001**, *13*, 3709.

(7) Coronado, E.; Galán-Mascarós, J.-R.; Gómez-García, C. J.; Laukhin, V. *Nature* **2000**, *408*, 447–449.

(8) Special Issue on Organic–Inorganic Nanocomposite Materials. *Chem. Mater.* **2001**, *13*.

(9) Lacroix, P. G.; Clément, R.; Nakatani, K.; Zyss, J.; Ledoux, L. *Science* **1994**, *263*, 658.

(10) Coradin, T.; Clément, R.; Lacroix, P. G.; Nakatani, K. *Chem. Mater.* **1996**, *8*, 2153.

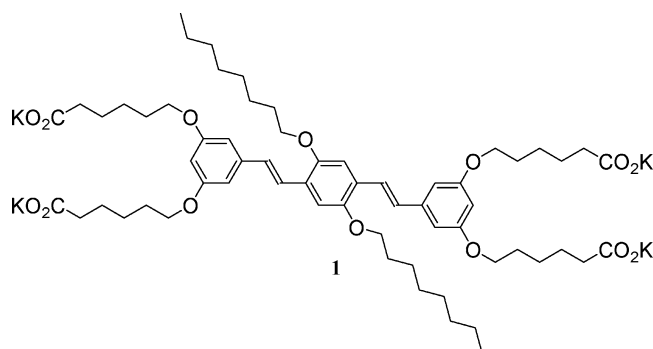
(11) Evans, J. S. O.; Bénard, S.; Yu, P.; Clément, R. *Chem. Mater.* **2001**, *13*, 3813–3816.

(12) Rabu, P.; Drillon, M.; Awaga, K.; Fujita, W.; Sekine, T. In *Magnetism: Molecules to Materials*; Miller, J. S., Drillon, M., Eds.; Wiley VCH: Weinheim, Germany, 2001, pp 357–395.

(13) Rabu, P.; Drillon, M. In *Handbook of Organic–Inorganic Hybrid Materials and Nanocomposites*; Nalwa, H. S., Ed.; American Scientific Publishers: Los Angeles, CA, 2003; Vol. 1, pp 297–351.

(14) Rabu, P.; Drillon, M. *Adv. Eng. Mater.* **2003**, *5* (4), 189–210.

Scheme 1



(trimers and tetramers).<sup>15</sup> It can also be added that OPV derivatives have been widely used for materials science applications such as light-emitting diodes (LEDs),<sup>16,17</sup> field effect transistors (FETs),<sup>18</sup> or photovoltaic cells.<sup>19,20</sup> Finally, OPV derivatives have characteristic features that make them also versatile photo- and/or electro-active components for the preparation of photochemical molecular devices.<sup>21–23</sup>

## Results and Discussion

**Synthesis.** The strategy employed for the synthesis of OPV derivative **1** (Scheme 1) is based upon Wittig–Horner type chemistry (Scheme 2). To this end, aldehyde **4** and bis-phosphonate **5** were prepared first (Scheme 2). Compound **5** was obtained in three steps from hydroquinone as described in the literature.<sup>24</sup> Benzaldehyde **4** was prepared by reaction of 3,5-dihydroxybenzyl alcohol (**2**) with ethyl 6-bromohexanoate in DMF at 80 °C in the presence of K<sub>2</sub>CO<sub>3</sub> followed by oxidation of the resulting benzylic alcohol **3** with MnO<sub>2</sub> in CH<sub>2</sub>Cl<sub>2</sub>.

Treatment of aldehyde **4** with bis-phosphonate **5** in THF in the presence of *t*-BuOK gave the OPV trimer **6**. It can be noted that the *E* configuration of the double bonds in **6** was confirmed by a coupling constant of ca. 17 Hz for the AB system corresponding to the vinylic protons in the <sup>1</sup>H NMR spectrum. Finally, the hydrolysis of the ethyl ester groups in **6** was achieved by treatment with an excess of KOH in H<sub>2</sub>O/THF followed by acidification with HCl. Tetracarboxylic acid **7** thus obtained was then converted into the corresponding potassium salt **1** used for the preparation of the targeted

O/I compound **8**.<sup>25</sup> The formation of the carboxylate **1** is inferred by the shift of the antisymmetrical C–OO vibration band toward the symmetrical one ( $\Delta\nu \approx 135$  cm<sup>−1</sup>) in the IR spectra compared to that of the acid **7**. Similarly the difference between the two characteristic absorption bands of the carboxylates in **8** indicates that the carboxylates coordinate the Ni(II) atoms, merely in a bidentate mode as  $\Delta\nu \approx 165$  cm<sup>−1</sup> is weak but slightly larger than in the potassium salt.<sup>26,27</sup>

**Characterization.** The standard characteristics of all the compounds are detailed in the Experimental Section. In addition, the product **8** was characterized by powder X-ray diffraction by using a D5000 (Cu K $\alpha_1$  = 1.540598 Å) Siemens diffractometer in the Bragg–Brentano geometry. Thermogravimetric analysis of the compound was performed with a Setaram TG-DTA 92 thermobalance up to 1000 K under air. Magnetic data ( $\chi(T)$ ,  $\chi_{ac}(T)$ ,  $M(H)$ ) were collected from a SQUID magnetometer (Quantum Design MPMSXL) covering the temperature and field ranges 2–300 K, 0–5 T, respectively. AC susceptibility measurements were performed in a 3.5 Oe alternative field (20 Hz). UV–Vis–NIR studies on solid powder samples were performed with a Perkin-Elmer Lambda 19 instrument (spectra recorded by reflection at room temperature with a resolution of 4 nm and a sampling rate of 480 nm/min). The temperature dependence of the photoluminescence (PL) was measured in a backward configuration. An HBO mercury lamp was used as UV excitation source. Its light was filtered by a UG 11 colored filter. The sample was cooled in a helium bath cryostat (OXFORD Instrument MD11) in which the temperature could be adjusted between 3 and 300 K. The emitted light was focused onto the entrance slit of a 27-cm spectrometer (Spex 270M) and detected by photodiode array camera.

**Structure.** The hybrid compound Ni(OPV(COO)<sub>4</sub>)<sub>0.45</sub>·(OH)<sub>0.2</sub>·2.6H<sub>2</sub>O was characterized by powder X-ray diffraction (XRD). The diffraction pattern shown in Figure 1 exhibits essentially a series of 00*l* harmonics, characteristic of a lamellar structure with low interplanar correlations, merely explained by the large size (~30 Å) and the flexibility of the −(CH<sub>2</sub>)<sub>5</sub>− subunits in the organic pillars. The interlayer distance *d* = 28.98 Å deduced from the diffraction data is consistent with a quasi perpendicular arrangement of the OPV tetracarboxylate anions connecting the Ni(II) based layers.

The UV reflection spectra of the OPV-based ligand **1** and that of the Ni/OPV compound **8** are compared in Figure 2, which corroborates the presence of the OPV moieties in the hybrid compound. In addition, the UV spectrum of **8** exhibits absorption bands at  $\lambda = 1194$  nm (<sup>3</sup>T<sub>2g</sub> → <sup>3</sup>A<sub>2g</sub>), 738 nm (<sup>1</sup>E<sub>g</sub> → <sup>3</sup>A<sub>2g</sub>), and 676 nm (<sup>3</sup>T<sub>1g</sub>(F) → <sup>3</sup>A<sub>2g</sub>), that are characteristic of Ni(II) ions in octahedral geometry with *Dq* ≈ 830 cm<sup>−1</sup>. The fact that the forbidden <sup>1</sup>E<sub>g</sub> transition is near the <sup>3</sup>T<sub>1g</sub> one suggests that *Dq/B* is near unity as in common octahedral systems.<sup>28,29</sup> Octahedral high spin configuration for the

(15) Narwark, O.; Meskers, S. C. J.; Peertz, R.; Thorn-Csányi, E.; Bässler, H. *Chem. Phys.* **2003**, *294*, 1–15.

(16) Burroughes, J. H.; Bradley, D. D. C.; Brown, A. R.; Marks, R. N.; Mackay, K.; Friend, R. H.; Burns, P. L.; Holmes, A. B. *Nature* **1990**, *347*, 539.

(17) Friend, R. H.; Gymer, R. W.; Holmes, A. B.; Burroughes, J. H.; Marks, R. N.; Taliani, C.; Bradley, D. D. C.; dos Santos, D. A.; Brédas, J. L.; Lögdun, M.; Salaneck, W. R. *Nature* **1999**, *397*, 121.

(18) Halls, J. J. M.; Walsh, C. A.; Greenham, N. C.; Marseglia, E. A.; Friend, R. H.; Moratti, S. C.; Holmes, A. B. *Nature* **1995**, *376*, 498.

(19) Eckert, J.-F.; Nicoud, J.-F.; Nierengarten, J.-F.; Liu, S.-G.; Echegoyen, L.; Barigelletti, F.; Armaroli, N.; Ouali, L.; Krasnikov V.; Hadzioannou, G. *J. Am. Chem. Soc.* **2000**, *122*, 7467–7479.

(20) Müllen, K.; Wegner, G. *Electronic Materials: The Oligomer Approach*; Wiley-VCH: Weinheim, Germany, 1998.

(21) Armaroli, N.; Eckert, J.-F.; Nierengarten, J.-F. *J. Chem. Soc. Chem. Comm.* **2000**, 2105–2106.

(22) Armaroli, N.; Accorsi, G.; Gisselbrecht, J.-P.; Gross, M.; Eckert, J.-F.; Nierengarten, J.-F. *New J. Chem.* **2003**, *27*, 1470–1478.

(23) Gutiérrez-Nava, M.; Nierengarten, H.; Masson, P.; Van Dorselaer, A.; Nierengarten, J.-F. *Tetrahedron Lett.* **2003**, *44*, 3043–3046.

(24) Gomez-Escalonilla, M. J.; Langa, F.; Rueff, J.-M.; Oswald, L.; Nierengarten, J.-F. *Tetrahedron Lett.* **2002**, *43*, 7507–7511.

(25) See the Experimental Section.

(26) Deacon, G. B.; Phillips, R. J. *Coord. Chem. Rev.* **1980**, *33*, 227–250.

(27) Nakamoto, K. *Infrared and Raman Spectra of Inorganic and Coordination Compounds*, 4th ed.; Wiley: New York, 1986.

(28) Lever, A. B. P. *Inorganic Electronic Spectroscopy*, 2nd ed.; Elsevier: Amsterdam, The Netherlands, 1984.

(29) Banci, L.; Bencini, A.; Benelli, C.; Gatteschi, D.; Zanchini, C. *Struct. Bonding* **1982**, *52*, 37.

Scheme 2

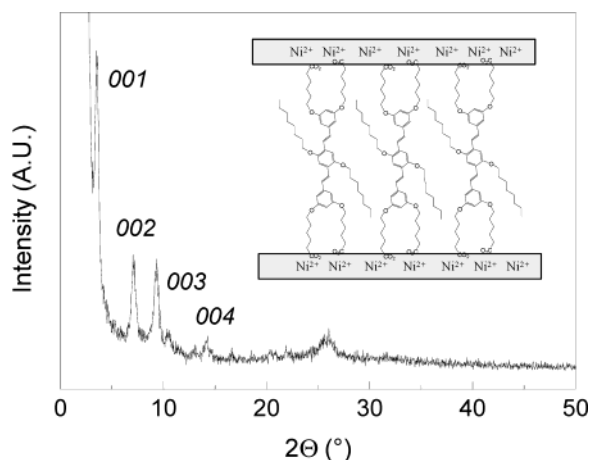
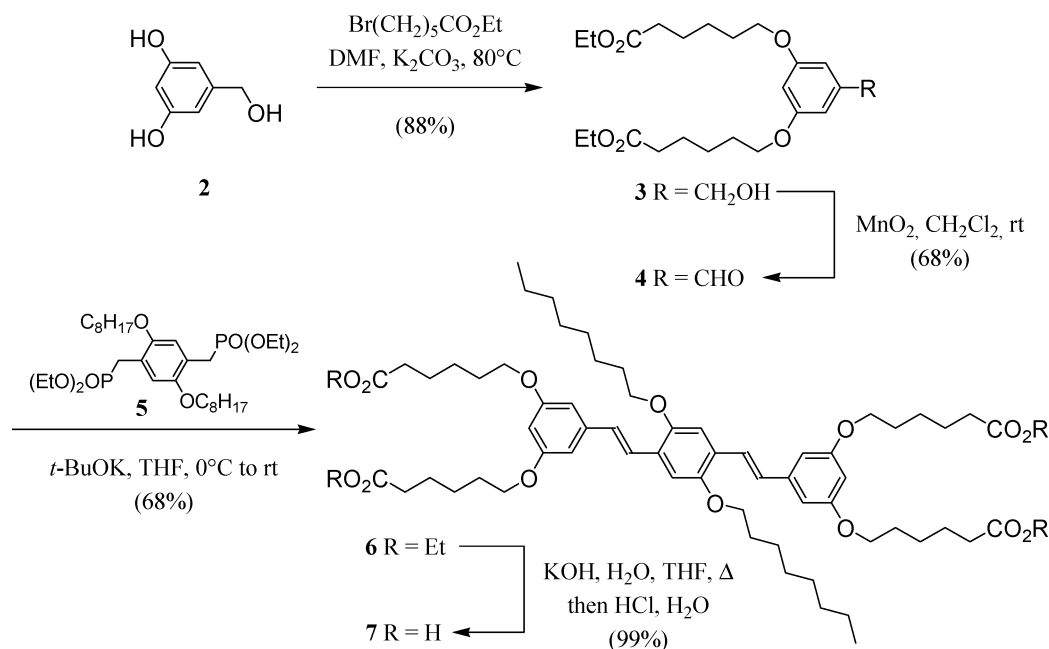


**Figure 1.** Powder XRD pattern of  $\text{Ni}(\text{OPV}(\text{COO})_4)_{0.45}(\text{OH})_{0.2} \cdot 2.6\text{H}_2\text{O}$  ( $\text{Cu K}\alpha_1 = 1.540598 \text{ \AA}$ ). A schematic structural model is given in the inset.

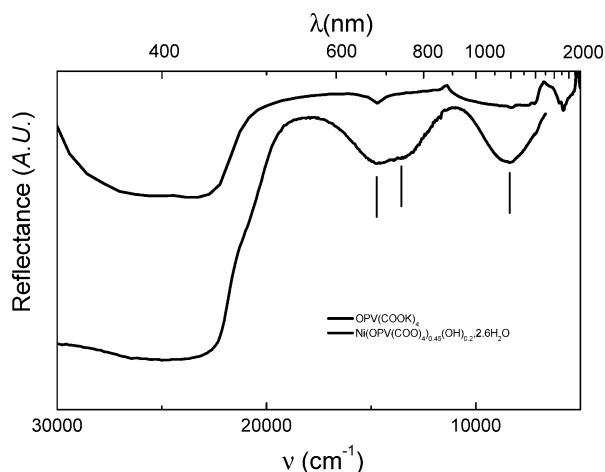


**Figure 2.** Solid-state UV spectra of the ligand **1** (above) and the compound **8** (below) at room temperature.

metal centers is also inferred from magnetic findings (see below).

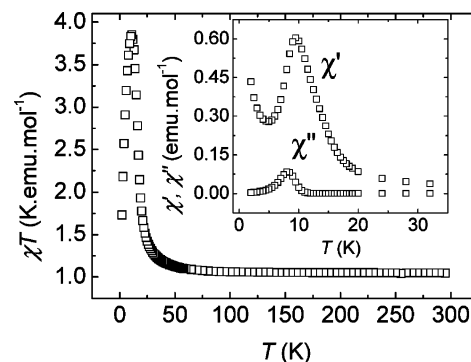


**Figure 3.** Magnetic susceptibility as  $\chi T$  vs  $T$  plot of  $\text{Ni}(\text{OPV}(\text{COO})_4)_{0.45}(\text{OH})_{0.2} \cdot 2.6\text{H}_2\text{O}$  measured under  $H = 500 \text{ Oe}$ . The ac susceptibility variation is shown in the inset.

**Magnetic Properties.** The magnetic properties of **8** are shown in Figure 3 as  $\chi T = f(T)$  and the variation of the ac magnetic susceptibility. The  $\chi T$  product fits well the Curie–Weiss law for  $T > 100 \text{ K}$  with  $C = 1.04 \text{ emu} \cdot \text{K} \cdot \text{mol}^{-1}$ , in agreement with the expected value for isolated  $\text{Ni}^{\text{II}}$  ions in Oh ligand field, and  $\theta = +1.5 \text{ K}$ , pointing to ferromagnetic interactions. Accordingly, the  $\chi T$  product is quasi constant ( $\sim 1.05 \text{ emu} \cdot \text{K} \cdot \text{mol}^{-1}$ ) from room temperature down to  $\sim 100 \text{ K}$ , then increases up to a maximum of  $3.85 \text{ emu} \cdot \text{K} \cdot \text{mol}^{-1}$  at  $11 \text{ K}$  and drops at lower temperature. The ac susceptibility measurements carried out under a  $20 \text{ Hz}/3.5 \text{ Oe}$  alternative field show a maximum of  $\chi'$  at  $9.5 \text{ K}$  followed by a slight increase below  $4 \text{ K}$ . In addition, the out-of-phase signal ( $\chi''$ ) exhibits a peak at  $8 \text{ K}$  (inset in Figure 3). The observed behavior agrees with in-plane ferromagnetic interactions and the onset of a 3D magnetic order ( $T_C = 9.5 \text{ K}$ ) which is confirmed by the hysteresis loop of the magnetization at low temperature ( $H_c = 425 \text{ Oe}$  at  $2 \text{ K}$ ). Note that complete saturation is not reached at  $H = 5 \text{ T}$  ( $M = 1.05 \mu_B$ ) pointing out the occurrence of a ferrimagnetic order (Figure 4).

The hybrid compound orders ferromagnetically although the distance between the magnetic layers is very large (ca.  $29 \text{ \AA}$ ). This result is well explained by the



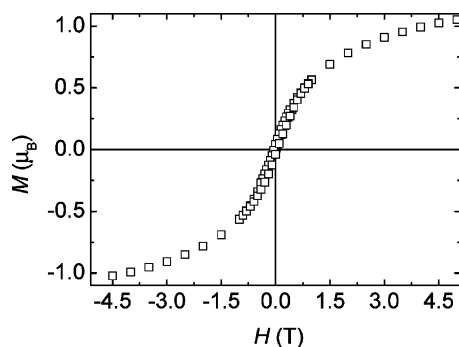


**Figure 4.** Magnetization versus field curve at 2 K for Ni(OPV(COO)<sub>0.45</sub>(OH)<sub>0.2</sub>·2.6H<sub>2</sub>O.

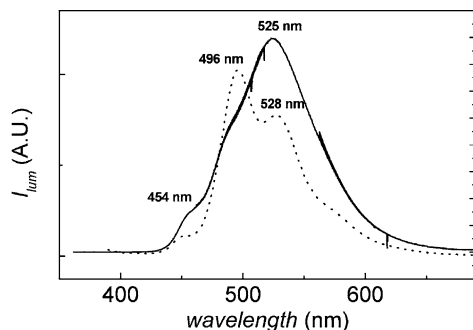


**Figure 5.** PL spectrum of solid Ni(OPV(COO)<sub>0.45</sub>(OH)<sub>0.2</sub>·2.6H<sub>2</sub>O at 200 K. The dotted line corresponds to the emission spectrum of the pure OPV-tetracarboxylate ligand **1** in the solid state ( $\lambda_{\text{exc}} = 375$  nm).

existence of dipolar interactions between the large moments arising in the layers as already established for a series of transition metal hydroxide based compounds where the layers are separated by large organic pillars.<sup>12,30</sup>

**Luminescence.** In solution, the emission spectrum of **1** exhibits a broad peak with a maximum at 429 nm in agreement with the values observed for the  $S_1 \rightarrow S_0$  emission band in similar *p*-phenylene-vinylene oligomers.<sup>15</sup> A vibronic structure is observed with peaks at 395 and 453 nm. The luminescent properties of the OPV moieties **1** inserted in compound **8** have been compared with those of the pure ligand in the solid state at room temperature (Figure 5). In the solid state, the maximum of luminescence of **1** is shifted to  $\lambda_{\text{max}} = 496$  nm with additional structures at 454 and 528 nm. Although quite large, this red shift of the emission bands could be explained by aggregation effects and deformation of the  $\pi$  system in the condensed phase compared to the ligand in dilute solution.<sup>15</sup> When grafted in the solid hybrid compound **8**, the maximum of luminescence is obtained at  $\lambda_{\text{max}} = 525$  nm at room temperature, whereas the vibronic features, although similar, are enlarged and result in a different profile. Such a difference is not very surprising considering the grafting of the OPV onto Ni(II) based inorganic layers may induce change in the vibrational structure of the chromophores together with slight reabsorption by the ligand (see Figure 2). The similarity between the solid-state emission spectra of the compounds **1** and **8** suggests strongly that the source of luminescence is really the OPV carboxylate rather

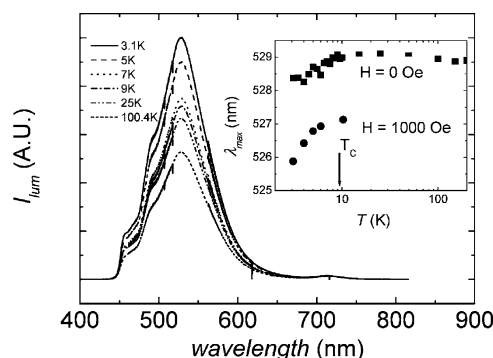


**Figure 6.** Variation of the photoluminescence spectra of Ni(OPV(COO)<sub>0.45</sub>(OH)<sub>0.2</sub>·2.6H<sub>2</sub>O with the temperature ranging between 3 and 300 K. The inset shows the corresponding variation of the position of the  $S_1 \leftarrow S_0$  band maximum in the magnetic field of the earth (squares) and in additional field of a magnet (circles).

than the nickel(II) centers, although partial energy transfer to the nickel ions cannot be ruled out by our data. It is worth noticing, however, that the results reported in the literature indicate that such energy transfer leads usually only to partial quenching and that, if any, luminescence of the Ni(II) centers is expected to occur in the Infrared rather than in the UV–vis range.<sup>31–33</sup>

To investigate the influence of the magnetic ordering on the photoluminescence of the OPV, we have recorded the shift of  $\lambda_{\text{max}}$  with temperature. Figure 6 shows that the shape of the photoluminescence spectrum is unchanged upon cooling from room temperature down to 3 K.

In turn, while  $\lambda_{\text{max}}$  is nearly constant between 200 and 10 K, a sharp decrease is observed below 10 K, which is precisely the onset of the ordering temperature. To confirm the influence of the magnetic order, a further experiment was carried out with a permanent magnet ( $H \approx 1000$  Oe) put near the sample. The same variation is observed below  $T_c$  with a slightly enhanced decrease of  $\lambda_{\text{max}}$  as shown by the different slopes of the  $\log(T)$  plots in insert of Figure 6.

It appears thus that the photoluminescence of the OPV ligand may be modified by the magnetic ordering of the inorganic Ni(II) layers. Although the effect is small, it is significant that it occurs at  $T_c$ . It is worth noting that the value of the applied field in our experiments was very weak and thus the system is far from exhibiting a large magnetization (cf. Figure 4). Further experiments using a larger magnetic field are needed to investigate this effect more precisely. The mechanism responsible for the interaction between the magnetic network and the  $\pi$  electron system of chromophores is still unclear. A Zeeman splitting of the electronic levels is ruled out because the transition occurs between spin singlets. In fact, the origin is likely the magnetostrictive effect occurring at the phase transition, which induces a change of the electronic structure of chromophores. The use of fluorescent molecules should give more insight on this mechanism. It remains that Ni(OPV-

(31) Fabbrizzi, L.; Foti, F.; Licchelli, M.; Poggi, A. *Inorg. Chem.* **2002**, *41* (18), 4612–4614.

(32) Wu, F. C.; Mills, R. B.; Evans, R. D.; Dillon, P. J. *Anal. Chem.* **2004**, *76* (1), 110–113.

(33) Stanley May, P.; Güdel, H. U. *J. Lumin.* **1990**, *46* (5), 277.

(30) Drillon, M.; Panissod, P. *J. Magn. Magn. Mater.* **1998**, *188*, 93.

$(\text{COO})_{4.45}(\text{OH})_{0.2} \cdot 2.6\text{H}_2\text{O}$  represents a rare example of a magnetoluminescent compound exhibiting a synergy between the optical and magnetic properties.

### Experimental Section

**General.** Reagents and solvents were purchased as reagent grade and used without further purification. Compound **5** was prepared according to the literature.<sup>24</sup> All reactions were performed in standard glassware under Ar. Evaporation and concentration were done at water-aspirator pressure and drying in vacuo at  $10^{-2}$  Torr. Column chromatography: silica gel 60 (230–400 mesh, 0.040–0.063 mm) from E. Merck. TLC: glass sheets coated with silica gel 60 F<sub>254</sub> from Merck; visualization by UV light. UV/Vis spectra ( $\lambda_{\text{max}}$  in nm ( $\epsilon$ )): Hitachi U-3000 spectrophotometer. IR spectra ( $\text{cm}^{-1}$ ): ATI Mattson Genesis Series FTIR instrument. NMR spectra: Bruker AC 200 (200 MHz); solvent peaks as reference;  $\delta$  in ppm,  $J$  in Hz. Elemental analyses were performed by the analytical service at the Institut Charles Sadron (Strasbourg, France).

**Compound 3.** A mixture of **2** (10.0 g, 71.4 mmol),  $\text{K}_2\text{CO}_3$  (38.2 g, 171 mmol), and 1-bromododecane (56.84 g, 228 mmol) in DMF (250 mL) was heated at 80 °C for 72 h. After the resulting mixture cooled, it was filtered and evaporated to dryness. The brown residue was taken up in  $\text{Et}_2\text{O}$ . The organic layer was washed with water, dried ( $\text{MgSO}_4$ ), filtered, and evaporated to dryness. Column chromatography ( $\text{SiO}_2$ ,  $\text{CH}_2\text{Cl}_2/\text{MeOH}$  98:2) gave **3** as colorless oil (26.6 g, 88%).  $^1\text{H}$  NMR (200 MHz,  $\text{CDCl}_3$ ): 1.22 (t,  $J = 7$  Hz, 6H), 1.50 (m, 4H), 1.74 (m, 8H), 2.33 (t,  $J = 7$  Hz, 4H), 3.94 (t,  $J = 7$  Hz, 4H), 4.03 (q,  $J = 7$  Hz, 4H), 4.61 (s, 2H), 6.35 (t,  $J = 2$  Hz, 1H), 6.49 (d,  $J = 2$  Hz, 2H).  $^{13}\text{C}$  NMR (50 MHz,  $\text{CDCl}_3$ ): 14.0, 24.5, 25.4, 28.7, 34.0, 60.1, 64.9, 67.4, 100.1, 104.8, 143.3, 160.1, 173.5. Anal. Calcd for  $\text{C}_{23}\text{H}_{36}\text{O}_7$  (424.5): C, 65.07; H, 8.55. Found: C, 64.96; H, 8.48.

**Compound 4.** A mixture of **3** (8.0 g, 18.8 mmol) and  $\text{MnO}_2$  (50 g) in  $\text{CH}_2\text{Cl}_2$  (100 mL) was stirred at room temperature for 4 h. After addition of  $\text{MgSO}_4$  (50 g), the mixture was filtered and the filtrate was evaporated to dryness. Column chromatography ( $\text{SiO}_2$ ,  $\text{CH}_2\text{Cl}_2/\text{MeOH}$  99:1) gave **4** (5.44 g, 68%) as a colorless oil.  $^1\text{H}$  NMR (200 MHz,  $\text{CDCl}_3$ ): 1.25 (t,  $J = 7$  Hz, 6H), 1.50 (m, 4H), 1.80 (m, 8H), 2.34 (t,  $J = 7$  Hz, 4H), 3.99 (t,  $J = 7$  Hz, 4H), 4.12 (q,  $J = 7$  Hz, 4H), 6.68 (t,  $J = 2$  Hz, 1H), 6.97 (d,  $J = 2$  Hz, 2H), 9.88 (s, 1H).  $^{13}\text{C}$  NMR (50 MHz,  $\text{CDCl}_3$ ): 14.2, 24.6, 25.5, 28.7, 34.2, 60.2, 68.0, 107.5, 107.9, 138.2, 160.6, 173.5, 192.0. Anal. Calcd for  $\text{C}_{23}\text{H}_{34}\text{O}_7$  (422.5): C, 65.38; H, 8.11. Found: C, 65.18; H, 8.03.

**Compound 6.** A solution of **4** (4.1 g, 9.7 mmol), **5** (2.9 g, 4.6 mmol), and  $t\text{-BuOK}$  (1.3 g, 11.6 mmol) in dry THF (45 mL) was stirred under Ar at room temperature for 2 h. A saturated aqueous solution of  $\text{NH}_4\text{Cl}$  was then added and the THF was evaporated. The aqueous layer was extracted twice with  $\text{CH}_2\text{Cl}_2$ . The organic layer was washed with water, dried ( $\text{MgSO}_4$ ), filtered, and evaporated to dryness. Column chromatography ( $\text{SiO}_2$ ,  $\text{CH}_2\text{Cl}_2/\text{AcOEt}$  96:4) gave **6** (3.9 g, 68%) as a yellow solid (mp 57 °C). IR (KBr): 1736 (asymC=O), 1593 (C=C). UV-vis ( $\text{CH}_2\text{Cl}_2$ ): 393 nm (42000), 327 (29000).  $^1\text{H}$  NMR (200 MHz,  $\text{CDCl}_3$ ): 0.88 (t,  $J = 6$  Hz, 6H), 1.26 (t,  $J = 7$  Hz, 12H), 1.50–1.85 (m, 48H), 2.35 (t,  $J = 7$  Hz, 8H), 3.99 (t,  $J = 7$  Hz, 8H),

4.01 (t,  $J = 7$  Hz, 4H), 4.12 (q,  $J = 7$  Hz, 8H), 6.37 (t,  $J = 2$  Hz, 2H), 6.67 (d,  $J = 2$  Hz, 4H), 7.05 (d,  $J = 17$  Hz, 2H), 7.09 (s, 2H), 7.41 (d,  $J = 17$  Hz, 2H).  $^{13}\text{C}$  NMR (50 MHz,  $\text{CDCl}_3$ ): 14.1, 14.2, 22.7, 24.7, 25.7, 26.3, 28.1, 29.0, 29.3, 29.5, 31.8, 34.3, 60.2, 67.7, 69.5, 100.7, 105.2, 110.9, 124.0, 126.8, 129.0, 139.9, 151.1, 160.3, 173.6. Anal. Calcd for  $\text{C}_{70}\text{H}_{106}\text{O}_{14}$  (1171.6): C, 71.76; H, 9.12. Found: C, 72.10; H, 9.18.

**Compound 7.** A mixture of **6** (2.0 g, 1.7 mmol) and KOH (1.2 g, 21.4 mmol, 5 mL) in THF/ $\text{H}_2\text{O}$  8:1 (45 mL) was refluxed for 24 h. After the mixture cooled, an aqueous 1 M solution of HCl was added and the THF was evaporated. The yellow precipitate was filtered and washed several times with water. The resulting solid was dissolved in acetone, dried ( $\text{MgSO}_4$ ), filtered, and evaporated to dryness to give **7** (1.69 g, 99%) as a yellow solid (mp 120 °C). IR (KBr): 3448 (O–H), 1705 (asymC=O), 1593 (C=C), 1423 (symC=O). UV-vis (DMSO): 397 (30000).  $^1\text{H}$  NMR (200 MHz,  $\text{DMSO}-d_6$ ): 0.81 (t,  $J = 6$  Hz, 6H), 1.50–1.85 (m, 48H), 2.22 (t,  $J = 7$  Hz, 8H), 3.96 (t,  $J = 7$  Hz, 8H), 4.05 (t,  $J = 7$  Hz, 4H), 6.38 (t,  $J = 2$  Hz, 2H), 6.65 (d,  $J = 2$  Hz, 4H), 7.29 (s, 2H), 7.32 (AB,  $J = 17$  Hz, 4H). Anal. Calcd for  $\text{C}_{62}\text{H}_{90}\text{O}_{14}$  (1059.4): C, 70.29; H, 8.56. Found: C, 70.23; H, 8.57.

**Compound 1.** An aqueous solution of KOH (0.212 g, 3.8 mmol,  $\text{H}_2\text{O}$  5 mL) was added dropwise to a solution of **7** (1.0 g, 0.9 mmol) in refluxing acetone (600 mL). After 3 h under reflux, the solution was cooled to room temperature and stirred at this temperature for 3 h. The yellow precipitate was filtered and washed several times with cold acetone then ethanol and dried under vacuum to give **1** (0.80 g, 70%) as a yellow solid (dec 200 °C). IR (KBr): 1558 (asymC=O), 1593 (C=C), 1423 (symC=O). UV-vis ( $\text{H}_2\text{O}$ ): 375 (18000), 324 (21000). Anal. Calcd for  $\text{C}_{62}\text{H}_{86}\text{O}_{14} \cdot 2\text{H}_2\text{O}$  (1247.8): C, 59.68; H, 7.27. Found: C, 59.73; H, 7.05.

**Compound 8,  $\text{Ni}(\text{OPV}(\text{COO})_{4.45}(\text{OH})_{0.2} \cdot 2.6\text{H}_2\text{O})$ .**  $\text{Ni}(\text{NO}_3)_2 \cdot 6\text{H}_2\text{O}$  (0.15 g, 0.5 mmol) in  $\text{H}_2\text{O}$  (3 mL) was added dropwise to a solution of  $\text{OPV}(\text{COOK})_4$  (0.3 g, 0.2 mmol) in  $\text{H}_2\text{O}$  (5 mL). An aqueous solution of KOH was then added to get pH ~9–10. The solution was stirred for 72 h. Ethanol (15 mL) was added and a yellow precipitate was formed. After filtration of the solution, the precipitate was washed several times with ethanol and dried overnight under vacuum. Compound **8** was obtained in a relatively good yield (>80%). The chemical formula was in agreement with the C and H content measured by chemical analysis, the Ni and water content deduced from thermal gravimetric analysis (TGA, combustion in air, 7.9% weight-loss at 130 °C, 83% weight-loss at 500 °C, NiO was identified by XRD of the final product) and with the magnetic finding ( $\mu_{\text{eff}} = 2.9 \mu_{\text{B}}/\text{Ni}^{\text{II}}$  at 300 K). IR (KBr): 1589 (asymC=O), 1423 (symC=O). Anal. Calcd for  $\text{NiC}_{27.9}\text{H}_{41.4}\text{O}_{9.1}$  (583.8): C, 57.39; H, 6.84; Ni, 10.0;  $\text{H}_2\text{O}$ , 8.02. Found: C, 57.78; H, 7.09; Ni, 13;  $\text{H}_2\text{O}$ , 7.9.

**Acknowledgment.** The CNRS and Université Louis Pasteur of Strasbourg, France, supported this work. A.D. thanks the French Ministry for Research and Technology for her PhD grant. The authors thank Guillaume Rogez, IPCMS, Strasbourg, France, for helpful discussion.

CM049792C